$$n^{(k)} := N\, S^{(k)} + 1$$

Consistently we have to assume that $n^{(k)} + 1 \equiv 0 \mod N$. Concerning the step $h^{(k)}$ for the k-th iteration, in this case we obtain

$$h^{(k)} = h^{(0)}\, \frac{1}{S^{(k)}} \tag{6.32}$$

Notice that $\beta \equiv \alpha + (n^{(k)} - 1)\, h^{(k)}$ as it is supposed to be. By construction it follows immediately that for every $k \in \mathbb{N}$ the relationship

$$h^{(k)} = \frac{S^{(k-1)}}{S^{(k)}}\, h^{(k-1)} \tag{6.33}$$

holds.

At this stage, interpolation of the given order N is performed on the subdivision $I_j^{(k)}$ containing τ, i.e. with $\tau \in I_j^{(k)}$. The error made in the k-th iteration is denoted with $\varepsilon^{(k)}$ and expressed in a natural way through

$$\varepsilon^{(k)} = \|F(\tau) - \overrightarrow{P}^{(k)}(\tau)\| \tag{6.34}$$

where $\overrightarrow{P}^{(k)}$ is the interpolating map corresponding to the k-th iteration.

Supposing the error $\varepsilon^{(k)}$ to have the form (to some extent, in a heuristic way)

$$\varepsilon^{(k)} = C\, \big(h^{(k)}\big)^p \qquad C > 0 \tag{6.35}$$

for every iteration k, we are left with the problem of establishing the exponent $p \in \mathbb{N}$ that expresses the order of convergence. For this purpose we compare the error relative to two consecutive iterations, that is we consider the ratio

$$\frac{\varepsilon^{(k-1)}}{\varepsilon^{(k)}} \tag{6.36}$$

which leads to the following equation

$$\frac{\varepsilon^{(k-1)}}{\varepsilon^{(k)}} = \left(\frac{h^{(k-1)}}{h^{(k)}}\right)^p = \left(\frac{S^{(k)}}{S^{(k-1)}}\right)^p \tag{6.37}$$

and hence to

$$\boxed{p = \frac{\ln\left(\dfrac{\varepsilon^{(k-1)}}{\varepsilon^{(k)}}\right)}{\ln\left(\dfrac{S^{(k)}}{S^{(k-1)}}\right)}} \tag{6.38}$$

6.2 Numerical Applications

In this section attention focuses more generally on the class of convex-valued maps taking the following form:

$$F :\ I \Longrightarrow \mathbb{R}^2 :\ t \mapsto A(t) \cdot U$$

Here $A(\cdot)$ is a matrix-function

$$A : I \longrightarrow \mathbb{R}^{2\times 2} \tag{6.39}$$

and U belongs to $\mathcal{C}(\mathbb{R}^2)$. We also consider the particular case of A coinciding with a scalar function $\lambda(\cdot)$. These classes, although remaining simple, are at the same time very indicative of the state-of-the-art.

At this stage, making use of the notation introduced in Section 2.2 and applying the recursive definition of the embedding J_2 as described in Section 3.2, $\overrightarrow{F}$ reads explicity

$$\begin{aligned}\overrightarrow{F}(t) = J_2\big(F(t)\big) &= \Big(J_1\big(F_{\perp}^{l_1}(t)\big), \delta^*(l_1, F(t))\Big)_{l_1\in S^1}\\ &= \Big(\delta^*(l_0, F_{\perp}^{l_1}(t)), \delta^*(l_1, F(t))\Big)_{l_0\in S^0, l_1\in S^1}\end{aligned}$$

Since the first component actually represents a directed interval, and therefore takes only two real values, the above expression can be rewritten (in the case of directed polytopes, see [Per03]) in an easier way with the aid of the scalar product as shown in [Per03]. Thus one has:

$$\overrightarrow{F}(t) = \begin{pmatrix} -\langle y(l,t), l^{\perp}\rangle \\ \langle y(l,t), l^{\perp}\rangle \\ \langle y(l,t), l\rangle \end{pmatrix} \quad \text{for all} \quad l \in S^1$$

where the point $y(l,t)$ is in the supporting face $Y\big(l, F(t)\big)$ in the direction l.

Some remarks for the particular case of $A(\cdot)$ in (6.39) coinciding with a scalar function $\lambda(\cdot)$ should be given. The image $\lambda(t)\cdot U$ remains convex for every $t \in I$. Furthermore, if it is assumed non-negative on the interval I, this former fact induces some simplification in the interpolation process. In fact, applying recursively Theorem 4.6 and Definition 4.5 the expression for the divided differences takes the following form

$$\begin{aligned}F[\Theta] &= \frac{F[\theta_1,\dots,\theta_k] - F[\theta_0,\dots,\theta_{k-1}]}{\theta_k - \theta_0}\\ &= \frac{\lambda[\theta_1,\dots,\theta_k] - \lambda[\theta_0,\dots,\theta_{k-1}]}{\theta_k - \theta_0}\cdot J_2\big(U\big) \quad \in \overrightarrow{\mathcal{D}}^2\end{aligned}$$

thus we obtain

$$F[\Theta] \equiv \lambda[\Theta]\cdot J_2\big(U\big)$$

From the above representation, it appears clear how the interpolation of $\overrightarrow{F}$ corresponds to the interpolation of its components. Concerning the interpolating polynomial, we have as a direct consequence of the above equation, the following relation

$$\mathcal{K}_{\Theta}F = \big(\mathcal{K}_{\Theta}\lambda\big)\cdot J_2(U)$$

Similarly concerning the error evaluation one has

$$\begin{aligned}\|\overrightarrow{F}(\tau) - \overrightarrow{P}(\tau)\| &= \big|\lambda(\tau) - \big(\mathcal{K}_{\Theta}\lambda\big)(\tau)\big|\ \|J_2\big(U\big)\|\\ &= \big|\lambda(\tau) - \big(\mathcal{K}_{\Theta}\lambda\big)(\tau)\big|\ \|U\|\end{aligned}$$

Remark 6.18 (Numerical Tests). Although simplifications as described above may be possible, we interpolate directly in the space $\overrightarrow{\mathcal{D}}^2$ and do not perform scalar interpolation in any of our numerical tests.

Remark 6.19. The above reasoning shows that, if the map F has the particular form $\lambda(t)\cdot J_2(U)$ then the interpolation of any order is possible just depending on the function $\lambda(t)$. For example, in the Numerical Test 6.23 interpolation of order up to 3 has been performed.

Geometrical Constraints

In [Lem95] conditions on the SVF F are required in order to achieve non-emptiness of the interpolating map for every $t \in I$. Therein the following condition is enunciated:

Condition 6.20. For every $t \in I$ the ball

$$B\big(m(t), r(t)\big) := \{x \in \mathbb{R}^n \ \mid \ \|x - m(t)\| \leq r(t)\}$$

with centre $m(t) \in \mathbb{R}^n$ and radius $r(t) > 0$ is contained entirely in the image $F(t)$.

As stated in [Lem95, Corollary 2.5], Condition 6.20 has to be set in order to guarantee the interpolating map to F to be non-empty and also when deriving error estimates. We also notice that in [Lem95], the support function $\delta^*(F(\cdot), l)$ of each image $F(t) \in \mathcal{C}(\mathbb{R}^n)$ is interpolated polynomially; nevertheless, the interpolating map as a whole is not in general polynomial (with respect to the parameter t) as a set-valued function. In our approach, a second component leading back to the supporting face is considered and interpolated as well; also because of this fact, the overall interpolating function $\mathcal{K}_\Theta F$ (always) has a polynomial form with respect to the parameter t. Moreover, the visualisation constitutes a main difference between the two approaches.

Performing Computer Calculation

The computations have been performed with the aid of the software tool *SVUPI*, a *C++* collection of classes, especially developed within the frame of the PhD thesis. A broad description of *SVUPI* is given in Chapter 7. An exhaustive description of the mentioned software is shown in the white paper [Per05]. In addition to the software *SVUPI*, the *C++* class collection implementing the *reduced representation* of the so called *directed polytopes*, has been deployed as well. A full description of it is to be found in [Per03].

Of course, due to the architecture of today's computers, some approximations had to be introduced. The use of *reduced representation*, certainly represents a first approximation since the images of the function $\overrightarrow{F}$ are approximated through means of directed polytopes. In practice, this fact corresponds to a discrete choice of directions. A further approximation is due to the computation of the norm of a directed set; again, we have to discretise the directions in the bundle.

Several examples have been set up and run on a Intel® Xeon™CPU 3.06 GHz based machine.

All computations have been done with double precision since in our case we do not see any indication for using arbitrarily precision tools like [CLN05], [LED05] or [GMP05].

6.2.1 Time Dependent Scaled 2-Dimensional Maps

The first bunch, Numerical Test 6.21 and Numerical Test 6.22, of presented computations does satisfy Condition 6.20 posed above whereas Numerical Test 6.23 does not. The examples portrayed in this section shows *inter alia* that no particular geometrical conditions on F have to be assumed in order to prevent the interpolating function from being eventually empty for some $t \in I$. What is more, the interpolating function is always polynomial with respect to t. Of course the first aim of the section consists in assessing numerically the order of convergence.

Expanding Ball

Numerical Test 6.21. *The convex-valued function F to be interpolated reads*

$$F : [0,1] \Longrightarrow \mathbb{R}^2 \; : \; t \mapsto \frac{1}{t+1} \cdot B(0,1) \tag{6.40}$$

Here $B(0,r)$ denotes as usual the ball centred in 0 with radius $r > 0$. By simply applying the definition, we may rewrite $F(t)$ in a more compact form as:

$$F(t) = B(0, \frac{1}{t+1}) \tag{6.41}$$

Clearly $F(t)$ is strongly convex for every t in $[0,1]$ (recall Definition 6.2). Incidentally, notice that F clearly satisfies Condition 6.20. Furthermore, from Section 3.3.1 we learn that F is directed-differentiable on the interval $[0,1]$.

Since the tests are focused on the numerical aspects of the directed interpolation, we do not give a full description of the embedding but just give the end result that reads:

$$\overrightarrow{F}(t) = J_2\big(\frac{1}{t+1} \cdot B(0,1)\big) = \big(\overrightarrow{0}\,, \frac{1}{t+1}\big)_{l \in S^1}$$

We incidentally mention that we actually need to embed only the unity ball and that the function $\overrightarrow{F}$ takes the following final form:

$$\begin{aligned} \overrightarrow{F}(t) &= \frac{1}{t+1} \cdot \overrightarrow{F}(0) \\ &= \frac{1}{t+1} \cdot J_2\big(B(0,1)\big) \end{aligned}$$

Numerical Results and Depiction of Numerical Test 6.21

Interpolation of 2nd degree of $\overrightarrow{F}$ has been performed on the knot grid below

$$\Theta := \{\, \theta_0 = 0.0\,,\, \theta_1 = 0.5\,,\, \theta_2 = 1.0 \,\}$$

obtaining the interpolating map

$$\begin{aligned} \mathcal{K}_\Theta F &= \left(\mathcal{K}_\Theta \frac{1}{t+1}\right) \cdot J_2\big(B(0,1)\big) \\ &= (\frac{1}{6}\,t^2 - \frac{2}{3}\,t + 1) \cdot \big(\overrightarrow{0}\,, 1\big)_{l \in S^1} \end{aligned}$$

Evaluation of $\overrightarrow{F}$ and of the interpolating map $\overrightarrow{P}(\cdot)$ has then been computed on the grid

$$T := \big\{\, \tau_0 = 0.166667\,,\, \tau_1 = 0.333333\,,\, \tau_2 = 0.666667\,,\, \tau_3 = 0.833333 \,\big\}$$

Figure 6.1 depicts the values taken from both $\overrightarrow{F}$ and $\overrightarrow{P}(\cdot)$ on T. Starting from the outer circle going towards the interior, the values $\overrightarrow{F}(\tau_j)$ and $\overrightarrow{P}(\tau_j)$ for $j = 0,1,2,3$ are shown. For enhanced optical readability, only the boundary without the bundle has been visualised.

Since we are dealing with a polynomial map of 2nd degree (in the sense of Chapter 5), only the divided differences

$$\int_{[\theta_0]} \mathrm{D}^0 \overrightarrow{F} \qquad \int_{[\theta_0,\theta_1]} \mathrm{D}^1 \overrightarrow{F} \qquad \int_{[\theta_0,\theta_1,\theta_2]} \mathrm{D}^2 \overrightarrow{F}$$

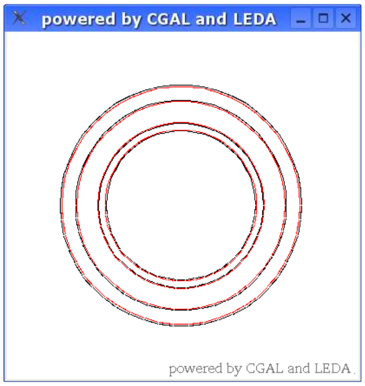

Fig. 6.1. $\overrightarrow{F}$ respectively $\overrightarrow{P}$ coloured respectively in black and in red evaluated on the grid T. Starting from the outer circle going towards the inside, the boundary (without the orientation bundle) is shown for τ_0, τ_1, τ_2 and τ_3.

of the 0, 1st, and 2nd order have to be computed. These have been depicted in Figure 6.2 coloured respectively in black, red and green. We emphasise an interesting fact. Not all of the divided differences are convex directed sets; namely, the one of 1st order (Figure 6.2, coloured in red) is a concave (for further details on the meaning of this expression refer to Section 2.2 and, of course, [BF01a], [BF01b] or [Per03]) directed set (visually this means that the directions in the bundle are oriented inwards). Nevertheless the overall result is convex, by which we mean that the interpolating map $\overrightarrow{P}(\cdot)$ can be obtained through embedding of a convex-valued function, precisely

$$\overrightarrow{P}(t) = J_2\big(V_2(\overrightarrow{P}(t))\big)$$

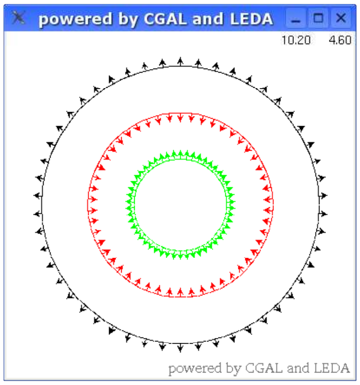

Fig. 6.2. The divided differences. The boundary and the orientation bundle of the divided differences of order $j = 1, 2, 3$ coloured respectively in black, in red, in green.

For assessing the speed of convergence (expressed by the value of the parameter p in Equation (6.38)) this numerical test has been carried out for 5 iterations (pay attention to the parameter k in the tables to come) following the scheme described in Section 6.1.2. As indicated by the values in the tables the order of convergence approaches the one theoretically expected (the original data is filed [Per06, `NumericalTest`]).

1st order interpolation

k-th iteration	S_k	ε_k	p
0	1	0.799604	–
1	4	0.228458	1.80736
2	16	0.0592291	1.94755
3	64	0.0149449	1.98665
4	256	0.00374426	1.99690

As indicated by the values in the tables the order of convergence approaches the one theoretically expected (the original data is filed [Per06, `NumericalTest`]).

2nd order interpolation

k-th iteration	S_k	ε_k	p
0	1	0.0125	–
1	10	3.95946e-05	2.49927
2	100	4.60648e-08	2.93427
3	1000	4.6793e-11	2.99319

Expanding Square

Numerical Test 6.22. *The convex-valued function F to be interpolated reads:*

$$F : [0,1] \Longrightarrow \mathbb{R}^2 \;:\; t \mapsto \frac{1}{t+1} \cdot [-1,1]^2 \tag{6.42}$$

For arbitrary $t \in I$ the convex and compact set $F(t)$ is described equivalently through the following equations:

$$F(t) = \Big[\frac{-1}{t+1}, \frac{1}{t+1}\Big]^2$$

The presented example may appear far too simple and very similar to the former in Numerical Test 6.21. However, the map F is not strongly convex (recall Definition 6.2). Nevertheless, the numerical tests assess a good order of convergence. Furthermore, F is directed-differentiable as an immediate consequence of Proposition 3.11.

In this case too, clearly F satisfies Condition 6.20. Passing on to the embedding, its expression reads (for further details on the computation of the embedding one may refer to [Per03, Chapter 3 & 4]):

$$\begin{aligned} \overrightarrow{F}(t) &= J_2\Big(\Big[\frac{-1}{t+1}, \frac{1}{t+1}\Big]^2\Big) \\ &= \frac{1}{t+1} \cdot \begin{cases} \Big(-\langle l^{\perp}, p_i\rangle, \langle l^{\perp}, p_i\rangle, 1\Big)_{l \in S^1} & : \ \sphericalangle l \in \big((i-1)\frac{\pi}{2}, i\frac{\pi}{2}\big) \\ \Big(1,1,1\Big)_{l \in S^1} & : \ \text{otherwise} \end{cases} \end{aligned}$$

Hereby, for simplicity with p_i, $i = 1, \dots, 4$, the points (in anticlockwise order)

$$p_2 = \begin{pmatrix} -1 \\ 1 \end{pmatrix} \quad p_1 = \begin{pmatrix} 1 \\ 1 \end{pmatrix}$$
$$p_3 = \begin{pmatrix} -1 \\ -1 \end{pmatrix} \quad p_4 = \begin{pmatrix} 1 \\ -1 \end{pmatrix}$$

have been denoted and (as in Section 3.4) with $\sphericalangle$ the function

$$\sphericalangle : S^{n-1} \longrightarrow [0, 2\pi) : l \mapsto \varphi$$

mapping the vector l to the angle φ with $l = (\cos\varphi, \sin\varphi)$.

Numerical Results of Numerical Test 6.22

We provide a comparison of two cases each corresponding to degree 1, 2. Notice the convergence order numerically determined as in Section 6.1.2 matches the expected theoretical value for the given order of interpolation (the original data is filed [Per06, `NumericalTest`]).

1st order interpolation

k-th iteration	S_k	ε_k	p
0	1	0.0833333	—
1	10	0.0021645	1.58546
2	100	2.46293e-05	1.94391
3	1000	2.49625e-07	1.99416

The original data is filed [Per06, `NumericalTest`].

2nd order interpolation

k-th iteration	S_k	ε_k	p
0	4	0.0999999	—
1	16	0.0285713	1.80736
2	64	0.00740729	1.94755
3	256	0.00186904	1.98665
4	1024	0.000468264	1.99690
5	4096	0.000117045	2.00026
6	16384	2.91754e-05	2.00423
7	65536	7.20413e-06	2.01786
8	262144	1.71105e-06	2.07394
9	1048576	3.37763e-07	2.34080

The original data is filed [Per06, `NumericalTest`].

3rd order interpolation

k-th iteration	S_k	ε_k	p
0	1	0.0023137	—
1	10	9.38957e-07	3.39166
2	100	1.13269e-10	3.91853
3	1000	1.16187e-14	3.98895

Point Expanding to a Segment

Numerical Test 6.23. *For a further test, we shall choose an apparently very simple convex-valued function, namely it reads:*

$$F : [0,1] \Longrightarrow \mathbb{R}^2 \;:\; t \mapsto (e^t - 1) \cdot \mathrm{co}\Big\{ \begin{pmatrix} 1 \\ 1 \end{pmatrix}, \begin{pmatrix} -1 \\ -1 \end{pmatrix} \Big\} \tag{6.43}$$

As well-known from the literature sources, this case hides difficulties. A geometrical representation of F is given by a segment arising from a point hence not solvable with the technique shown for example in [Lem95]. The constraint required in Condition 6.20 is harmed twice: $F(t)$ is a point for $t = 0$; secondly, $F(t)$ is a segment (for every t) hence no ball can be contained in it. Moreover, the map F is not strongly convex (recall Definition 6.2). Nervetheless, we are able to reach a good order of convergence.

Numerical Results of Numerical Test 6.23

In the following tables the results of the numerical tests for the interpolation of order 1, 2 and 3 are gathered starting, of course, with the order one. The data for 1st order interpolation is gathered in ([Per06, `NumericalTest`]):

1st order interpolation

k-th iteration	S_k	ε_k	p
0	1	1.68654	—
1	2	0.616978	1.45077
2	4	0.252282	1.29018
3	8	0.101405	1.31491
4	16	0.0327511	1.63052

whereas for the 2nd order in [Per06, `NumericalTest`]:

2nd order interpolation

k-th iteration	S_k	ε_k	p
0	1	0.0138966	—
1	10	2.03303e-05	2.83477
2	100	2.11439e-08	2.98296
3	1000	2.12272e-11	2.99829
4	10000	2.15383e-14	2.99368

Finally, for the 3rd order the numerical tests deliver (the data is filed [Per06, `NumericalTest`]):

3rd order interpolation

k	S_k	ε_k	p
0	1	0.00584869	—
1	10	1.02555e-06	3.75610
2	100	1.08707e-10	3.97470
3	1000	1.19904e-14	3.95742

6.2.2 Linearly Transformed Ellipse

In the former Section 6.2 the simple, but nevertheless very significant, case of the matrix $A(t)$ in Equation (6.39) coinciding with a scalar function has been investigated. At this stage we consider a more general case.

Numerical Test 6.24. *We give a quite close look at the convex-valued function obatined by letting an ellipse rotate. Thus we have:*

$$F: \ [0,1] \Longrightarrow \mathbb{R}^2 : \ t \mapsto A(t) \cdot B(0,1) \tag{6.44}$$

Hereby $B(0,1)$ *denotes, as usual, the unit ball and* $A(\cdot)$ *stands for the function-matrix below defining an expansion and a rotation of* $B(0,1)$*:*

$$A(t) := \begin{pmatrix} \cos\varphi t & -\sin\varphi t \\ \sin\varphi t & \cos\varphi t \end{pmatrix} \begin{pmatrix} 2 & 0 \\ 0 & 1 \end{pmatrix}$$

From Proposition 6.3 we learn that the images $F(t)$ are strongly convex sets for every $t \in [0,1]$. Concerning the differentiability of F we first point out that the function-matrix $A(\cdot)$ is clearly smooth. Therefore due to Proposition 3.13 the map F is convex-valued and directed-differentiable on the interval $[0,1]$.

Numerical Results of Numerical Test 6.24

As suggested by the values in the tables the convergence order approaches the one theoretically expected (the original data is filed [Per06, `NumericalTest`]).

1st order interpolation			
k-th iteration	S_k	ε_k	p
0	2	1.94357	–
1	4	1.66434	0.223763
2	8	0.940015	0.824192
3	16	0.399897	1.233050
4	32	0.122141	1.711080

2nd order interpolation			
k-th iteration	S_k	ε_k	p
0	1	1.12846	–
1	2	2.05884	-0.867475
2	4	1.26734	0.700033
3	8	0.20406	2.634740

Example 6.25. In Figure 6.3 to 6.5, the point $\tau \in I \setminus \Theta$ is considered. The interpolating map $\mathcal{K}_\Theta F$ of 2nd order is (visually) compared in $\tau \in I \setminus \Theta$ with the reference set-valued function F for different iterations (recall Section 6.1.2). The visualisations

$$V_2\Big(\big(\mathcal{K}_\Theta F\big)(\tau)\Big) \qquad \text{and} \qquad F(\tau) = V_2\Big(\overrightarrow{F}\,(\tau)\Big)$$

are depicted in the sequence below respectively in black and in red for three different iterations.

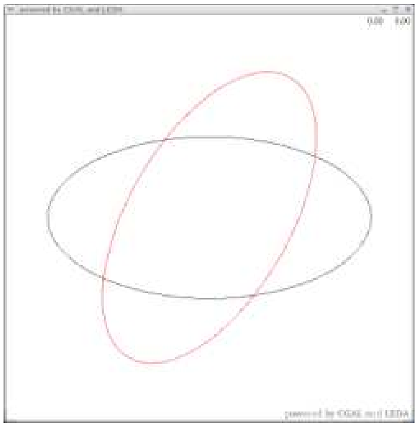

Fig. 6.3. $\tau = 0.33333$, 2nd order, 1-st iteration; reference $F(\tau)$ shown in red, $\big(\mathcal{K}_\Theta F\big)(\tau)$ shown in black.

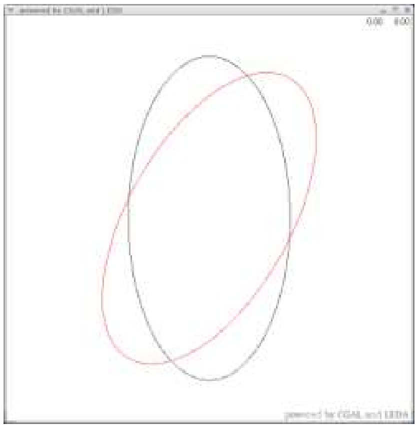

Fig. 6.4. $\tau = 0.33333$, 2nd order, 2-nd iteration; reference $F(\tau)$ shown in red, $\big(\mathcal{K}_\Theta F\big)(\tau)$ shown in black.

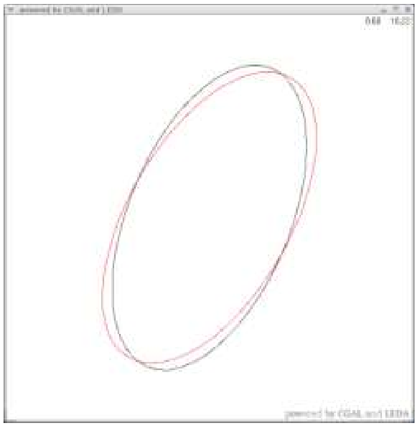

Fig. 6.5. $\tau = 0.33333$, 2nd order, 4-th iteration; reference $F(\tau)$ shown in red, $\big(\mathcal{K}_\Theta F\big)(\tau)$ shown in black.

The depictions in Example 6.25 (see Figure 6.3 to 6.5) suggest that if the number of iterations is increased (recall Section 6.1.2), while leaving the order of interpolation unchanged, a better visual result is reached.

Visual Behaviour of the Remainder

In this section we shift perspective and focus on the visualisation of the remainder

$$\mathcal{R}(\tau) := \overrightarrow{F}(\tau) - \big(\mathcal{K}_\Theta F\big)(\tau)$$

We interpolate the convex-valued function defined by

$$F_\mu :\ [0,1] \Longrightarrow \mathbb{R}^2 :\ t \mapsto A(t) \cdot Q_\mu$$

where Q_μ is the regular polytope defined in Numerical Test 6.26; two different choices for the function-matrix $A(\cdot)$ are then surveyed.

Numerical Test 6.32. *The matrix-function to be considered reads:*

$$A(t) := \begin{pmatrix} \cos\varphi t & -\sin\varphi t \\ \sin\varphi t & \cos\varphi t \end{pmatrix} \begin{pmatrix} 2 & 0 \\ 0 & 1 \end{pmatrix} \tag{6.45}$$

Picture 6.20 through 6.26 depict the visualisations obtained for this case.

Numerical Test 6.33. *The matrix-function considered reads:*

$$A(t) := \begin{pmatrix} e^t & 0 \\ 0 & t^5 + 1 \end{pmatrix} \tag{6.46}$$

The visualisation corresponding to this case are given in Picture 6.27 through 6.42.

We perform interpolation of degree $n = 2$ on the interval $I := [0,1]$ and evaluate the remainder in a specified point $\tau \in I$. We investigate the behaviour of the remainder when increasing the number of sides μ; this action corresponds to a smoothing of the involved SVF.

We observe that in the first case (see Picture 6.20 to Picture 6.26) the remainder appears not to shrink to a point as the parameter μ increases whereas in the second case this seems to be the case (see Picture 6.27 to Picture 6.32).

Picture 6.33 to 6.42 have been genereted leaving the increment h decrease (following the scheme described in Section 6.1.2) while leaving the parameter μ fixed instead.

The reference function $\overrightarrow{F}$ is plotted in black, the interpolating map $\mathcal{K}_\Theta F$ in red and the remainder in green. For enhanced readability the orientation bundle of the visualised sets is not shown.

Example 6.34. Second order interpolation of the convex-valued map F_μ, for $A(\cdot)$ as in Numerical Test 6.32, has been performed on the interval $[0, 1]$.

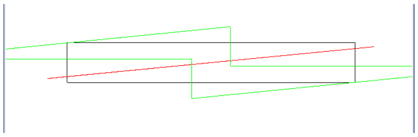

Fig. 6.20. $F_2(\tau)$, $\big(K_\Theta F_2\big)(\tau)$, $\mathcal{R}(\tau)$, $\tau = 0.03125$, 2nd order

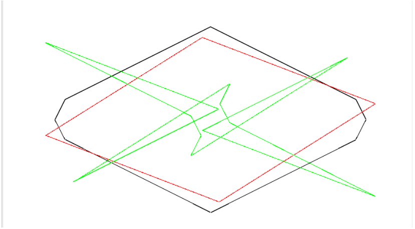

Fig. 6.21. $F_4(\tau)$, $\big(K_\Theta F_4\big)(\tau)$, $\mathcal{R}(\tau)$, $\tau = 0.03125$, 2nd order

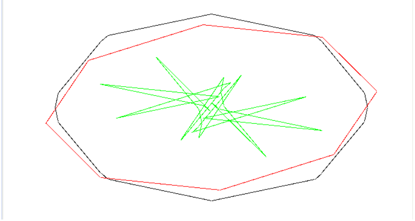

Fig. 6.22. $F_8(\tau)$, $\big(K_\Theta F_8\big)(\tau)$, $\mathcal{R}(\tau)$, $\tau = 0.03125$, 2nd order

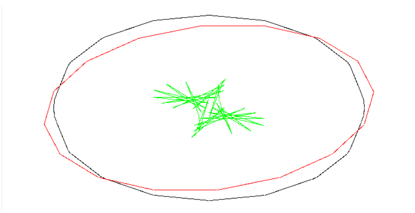

Fig. 6.23. $F_{16}(\tau)$, $\big(K_\Theta F_{16}\big)(\tau)$, $\mathcal{R}(\tau)$, $\tau = 0.03125$, 2nd order

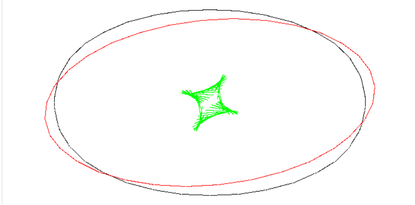

Fig. 6.24. $F_{32}(\tau)$, $\big(K_\Theta F_{32}\big)(\tau)$, $\mathcal{R}(\tau)$, $\tau = 0.03125$, 2nd order

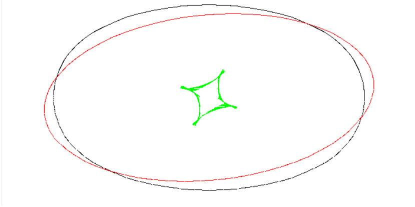

Fig. 6.25. $F_{64}(\tau)$, $\big(K_\Theta F_{64}\big)(\tau)$, $\mathcal{R}(\tau)$, $\tau = 0.03125$, 2nd order

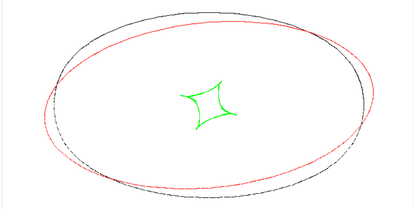

Fig. 6.26. $F_{128}(\tau)$, $\big(K_\Theta F_{128}\big)(\tau)$, $\mathcal{R}(\tau)$, $\tau = 0.03125$, 2nd order

Example 6.34: interpolation of 2nd order.

Example 6.35. For this set of visualisations, the convex-valued map F_μ with $A(\cdot)$ as in Numerical Test 6.33, has been considered. The map F_μ has been interpolated on the interval $[0,1]$.

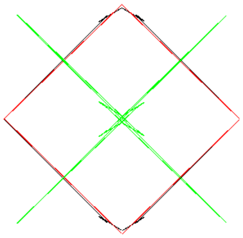

Fig. 6.27. $F_4(\tau)$, $\big(K_\Theta F_4\big)(\tau)$, $\mathcal{R}(\tau)$, $\tau = 0.03125$, 2nd order

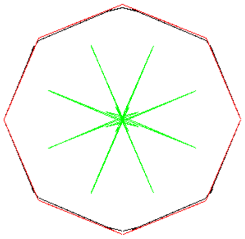

Fig. 6.28. $F_8(\tau)$, $\big(K_\Theta F_8\big)(\tau)$, $\mathcal{R}(\tau)$, $\tau = 0.03125$, 2nd order

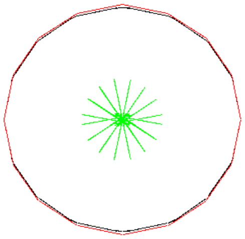

Fig. 6.29. $F_{16}(\tau)$, $\big(K_\Theta F_{16}\big)(\tau)$, $\mathcal{R}(\tau)$, $\tau = 0.03125$, 2nd order

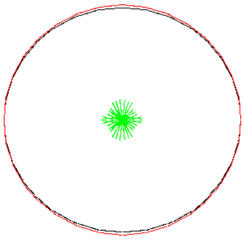

Fig. 6.30. $F_{32}(\tau)$, $\big(K_\Theta F_{32}\big)(\tau)$, $\mathcal{R}(\tau)$, $\tau = 0.03125$, 2nd order

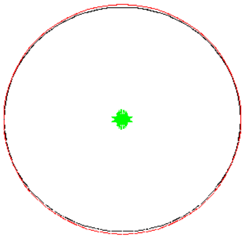

Fig. 6.31. $F_{64}(\tau)$, $\big(K_\Theta F_{64}\big)(\tau)$, $\mathcal{R}(\tau)$, $\tau = 0.03125$, 2nd order

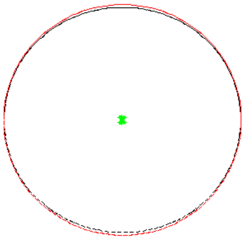

Fig. 6.32. $F_{128}(\tau)$, $\big(K_\Theta F_{128}\big)(\tau)$, $\mathcal{R}(\tau)$, $\tau = 0.03125$, 2nd order

Example 6.35: interpolation of 2nd order.

Example 6.36. We now change perspective and shrink the interpolation interval I_k containing τ by increasing the number of subdivision S_k as it has been described in Section 6.1.2. The matrix $A(t)$ as in Numerical Test 6.32 has been considered. [1]

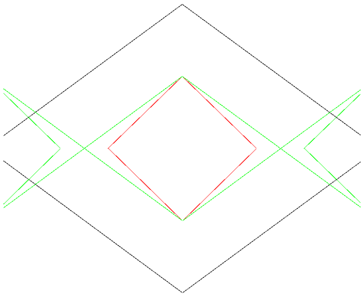

Fig. 6.33. $S_k = 1$, $F_4(\tau)$, $\big(K_\Theta F_4\big)(\tau)$, $\mathcal{R}(\tau)$, $\tau = 0.03125$, 2nd order

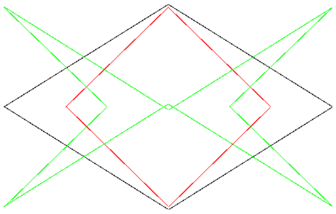

Fig. 6.34. $S_k = 2$, $F_4(\tau)$, $\big(K_\Theta F_4\big)(\tau)$, $\mathcal{R}(\tau)$, $\tau = 0.03125$, 2nd order

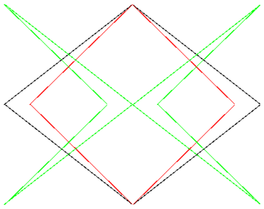

Fig. 6.35. $S_k = 4$,$F_4(\tau)$, $\big(K_\Theta F_4\big)(\tau)$, $\mathcal{R}(\tau)$, $\tau = 0.03125$, 2nd order

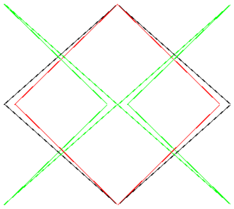

Fig. 6.36. $S_k = 8$, $F_4(\tau)$, $\big(K_\Theta F_4\big)(\tau)$, $\mathcal{R}(\tau)$, $\tau = 0.03125$, 2nd order

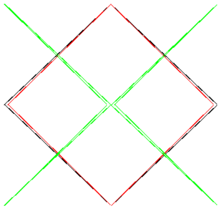

Fig. 6.37. $S_k = 16$, $F_4(\tau)$, $\big(K_\Theta F_4\big)(\tau)$, $\mathcal{R}(\tau)$, $\tau = 0.03125$, 2nd order

Example 6.36: interpolation of 2nd order.

[1] Please note that the picture shown in the upper-left corner had to be truncated.

Example 6.37. We proceed like in Example 6.36 with the choice for the matrix $A(t)$ given by Numerical Test 6.33. [2]

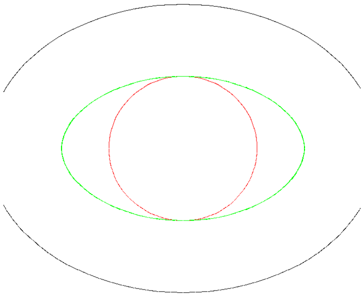

Fig. 6.38. $S_k = 1$, $F_{100}(\tau)$, $\big(K_\Theta F_{100}\big)(\tau)$, $\mathcal{R}(\tau)$, $\tau = 0.03125$, 2nd order

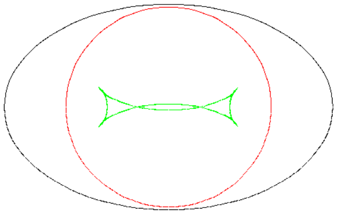

Fig. 6.39. $S_k = 2$, $F_{100}(\tau)$, $\big(K_\Theta F_{100}\big)(\tau)$, $\mathcal{R}(\tau)$, $\tau = 0.03125$, 2nd order

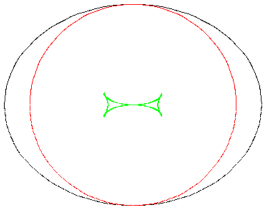

Fig. 6.40. $S_k = 4$, $F_{100}(\tau)$, $\big(K_\Theta F_{100}\big)(\tau)$, $\mathcal{R}(\tau)$, $\tau = 0.03125$, 2nd order

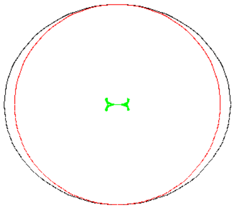

Fig. 6.41. $S_k = 8$, $F_{100}(\tau)$, $\big(K_\Theta F_{100}\big)(\tau)$, $\mathcal{R}(\tau)$, $\tau = 0.03125$, 2nd order

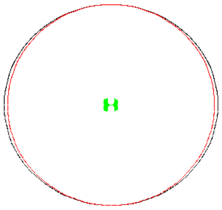

Fig. 6.42. $S_k = 16$, $F_{100}(\tau)$, $\big(K_\Theta F_{100}\big)(\tau)$, $\mathcal{R}(\tau)$, $\tau = 0.03125$, 2nd order

Example 6.37: interpolation of 2nd order.

[2] Please note that the first picture shown had to be truncated in order to leave proportion unaltered.